Isothermal Nanocalorimetry of Isotactic Polypropylene

Felice De Santis,*,† Sergey Adamovsky,‡ Giuseppe Titomanlio,† and Christoph Schick‡

Department of Chemical and Food Engineering, University of Salerno, 84084 Fisciano (SA), Italy, and Institute of Physics, University of Rostock, 18051 Rostock, Germany

Received July 6, 2007; Revised Manuscript Received September 18, 2007

ABSTRACT: A wide set of crystallization isotherms and the subsequent melting behavior of isotactic polypropylene (i-PP) were investigated using differential scanning calorimetry and nanocalorimetry with a very high rate in the cooling step. The latter technique offers, indeed, the distinct possibility to perform isothermal crystallization experiments at any temperature in between the glass transition and melting, as the test temperature can be reached at a cooling rate of 1000 K/s, thus, preventing crystallization during the cooling step. Isothermal tests after such fast cooling were performed at intervals of 5 K within the temperature range −15 to 90 °C, and a local exothermal overheating was observed. In particular, for each isotherm, the observed peaks were fitted using the Kolmogorov−Johnson−Mehl−Avrami model. The plot of the crystallization kinetics constant as function of temperature gives clear evidence of two kinetic processes. The subsequent heating scan performed starting from −15 °C showed an exothermic event, between 0 and 30 °C, due to the mesophase cold crystallization, for isotherms at a temperature lower than 20 °C.

Introduction

Since the invention of polypropylene (1954), which was rewarded with a Nobel prize to Natta and Ziegler, the use of polymers in everyday life has steadily increased. It still does due to successful research aimed at producing products with desired mechanical and chemical properties, tailored for a specific use (food containers, parts of car bodies, parts of prosthesis for the human body, components of composite material, etc.). Isotactic polypropylene (i-PP) has grown to a commodity polymer with numerous grades for specific end uses. At present, the physical properties of polypropylene should be tailored to the requirements with respect to processing and structure.

Solidification of semicrystalline polymers is largely influenced by the mobility of the chains in the melt and by the way crystalline structures are generated entrapping large fractions of the amorphous phase. The particular morphology of semicrystalline polymers is responsible for quite a peculiar behavior in the nucleation and growth of crystals. Such structures are called spherulites, because after nucleation they grow radially in quiescent condition, with the crystalline elements having elongated shapes (lamellae), roughly disposed along radii, with occasional branching.[1] Because of the amorphous inclusion, complete crystallization can never be achieved.

Furthermore, i-PP includes a peculiar polymorphism: when crystallized from the melt, the i-PP chains can organize several spatial arrangements giving rise to three different crystalline polymorphs, α-monoclinic, β-hexagonal, and γ-triclinic.[2−4] This is a peculiar feature with relevant consequences on the way the solidification process develops and on the mechanical properties of the final product.[5]

Moreover, when i-PP is quenched from the melt to low temperature, also the mesomorphic phase, an order intermediate between the amorphous and the crystalline phase is obtained. Although the mesomorphic phase[6] is known in the literature for a long time (sometimes denoted with different names like smectic,[7] paracrystal,[8] or glass[9]) and usually obtained in the i-PP processing, the related crystallization kinetics is rarely investigated with tailored experiments.

Titomanlio and co-workers[10,11] investigated the effect of the cooling rate on crystallization: thin films were quenched and cooling thermal histories were carefully monitored. Moreover, phase distribution of final i-PP samples,[10] after quenching over a wide range of cooling rates, was estimated by a deconvolution procedure applied to wide-angle X-ray scattering (WAXS) spectra. The analysis of quenched samples, however, does not reveal when the crystallization process toward the mesomorphic phase takes place; this cannot be monitored by conventional calorimetry, which is used to study temperature-activated processes, like crystallization, during temperature scans at cooling rates up to 1−8 K/s,[12,13] as at these cooling rates the mesomorphic phase does not form.

The heating rate of calorimeters is generally limited by the heat capacity of the sample and the addenda, the thermal conductivity and the thickness of the sample, the maximum power transferred to the system, and the speed of temperature measurement.[14] Recently developed quasi-adiabatic nanocalorimeters can operate at very high heating rates[15−20] because of very small addenda and sample heat capacities. The cooling rate, which is not controlled for the quasi-adiabatic systems, is limited by total heat capacity, sample size, and heat losses.[15,19] A thin film nanocalorimeter under nonadiabatic conditions allows cooling as well as heating rates of more than 10 000 K/s and, thus, allows for monitoring the crystallization of polymers in cooling ranges never explored earlier.[15,19]

Only recently,[20] a wide set of cooling scans, and subsequent melting behavior, of isotactic polypropylene (i-PP) were performed using nanocalorimetry at very high cooling rates. This technique offers, indeed, the distinct possibility to perform heat capacity measurements at rates of more than 1000 K/s, both in cooling and in heating, to characterize the crystallization. When the i-PP sample was solidified with a cooling rate larger than 160 K/s, an enthalpic process, related to the mesomorphic phase formation, was observed. Furthermore, at cooling rates higher than 1000 K/s, the i-PP sample did not crystallize in the α nor

* To whom correspondence should be addressed. E-mail: fedesantis@unisa.it.
† University of Salerno.
‡ University of Rostock.

10.1021/ma071491b CCC: $37.00
Published on Web 11/10/2007

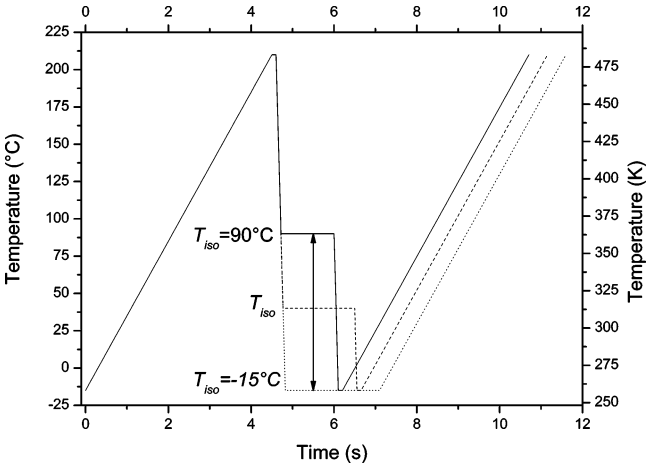

Figure 1. Experimental protocol; during the cooling steps the cooling rate was programmed to be 1000 K/s. Heating rate was 50 K/s.

in the mesomorphic form. The subsequent heating scan starting from −15 °C showed an exothermic event, between 0 and 30 °C, ascribed to the mesophase cold crystallization.

In this paper, the crystallization kinetics under quiescent conditions from the melt and subsequent melting behavior of i-PP is thoroughly investigated using standard differential scanning calorimetry and nanocalorimetry at isothermal conditions.

Experimental Section

The i-PP grade adopted in this study was supplied by Montell (now Basell), and its commercial name is T30G (non-nucleated, $M_w = 376\,000$, $M_w/M_n = 6.7$, tacticity = 87.6%). The crystallization of the same resin was the object of several studies.[10,20−23] Furthermore, the description of the same apparatus adopted for the nanocalorimetry experiments at high cooling rates on the same resin is available in ref 20. All measurements were carried out under a nitrogen atmosphere to prevent oxidative degradation of the sample.

A small i-PP sample was cut from a pellet under a microscope and placed very carefully onto the center of the sensor membrane, as described in refs 15, 17, and 18. An electric current was than applied to the heater to melt the sample and to attach it directly on the membrane of the sensor, without any sample holder. The sample of the order of 100 ng becomes a droplet of 60−80 μm diameter, while the thickness is 10−20 μm. One sample, exactly the same as adopted in ref 20, was prepared, and about 200 experiments were performed with this single sample. From the heat balance, taking into account the power needed to heat the sample and addenda at the given rate, heat losses to the surroundings as well as the electrical power applied to the heater, the total heat capacity can be obtained.[15] Addenda heat capacity of the order of 150 nJ/K was not subtracted because the same sensor and the same sample were used for all experiments discussed here. The uncertainty of the heat capacity measurement is about 20% while the reproducibility is much better. Sample mass was not independently determined and therefore apparent heat capacity and not specific heat capacity is given.

Tests were performed adopting the experimental protocols schematically shown in Figure 1; in particular, the sample was heated at 50 K/s from −15 to 210 °C and held at this temperature for 0.1 s. Larger times at the maximum temperature or/and higher maximum temperatures have to be avoided, because of the sample spreading out on the sensor surface. The sample was then cooled to the isothermal test temperature with a rate of 1000 K/s, and after cooling it was maintained at this temperature for the time required for crystallization. The cooling rate of 1000 K/s before the isothermal step is adopted because it is found capable to keep the sample amorphous.[20] Isothermal tests were performed each 5 K interval within the temperature range −15 to 90 °C. The sample

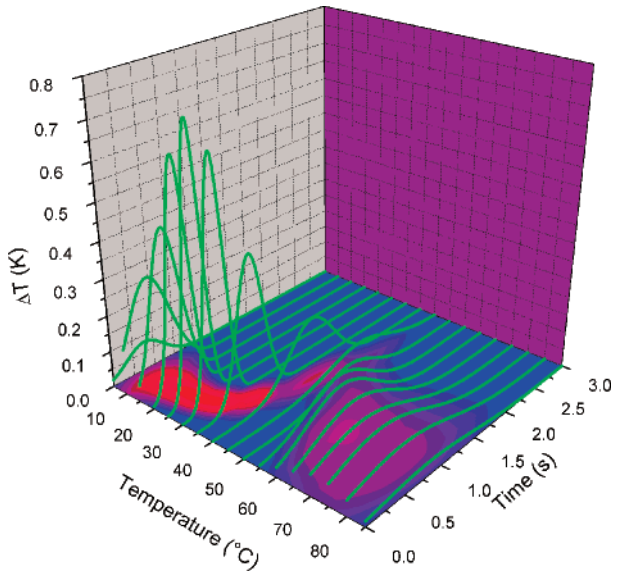

Figure 2. Temperature increase evolution vs time for each isothermal test.

was then cooled to −15 °C at the rate of 1000 K/s, and after cooling it was maintained at this temperature for 0.1 s. The sample, after being held 0.1 s at −15 °C, was heated again in the nanocalorimeter to 210 °C at 50 K/s.

Reproducibility was recurrently tested, and differences in the thermograms were negligible. Therefore, degradation and geometrical changes were considered negligible, also because the sample was held at temperatures above the melting temperature for only about 0.2 s during each experiment.

Results and Discussion

Isothermal Tests. After melting at 210 °C, the i-PP sample was investigated in a wide range of isothermal crystallization tests (−15 to 90 °C). During the isothermal tests, performed in the temperature range 5 to 85 °C, a local overheating in the temperature evolution was observed in the isothermal step due to the release of the crystallization enthalpy.

Isothermal crystallization of i-PP was explored in a large range of temperatures only recently;[24−26] very low temperatures isotherms were performed thanks to the considerable cooling rate before the isothermal step and the short time constant of the nanocalorimeter. For the isothermal tests performed in this work, at temperatures higher than 85 °C or lower than 5 °C any local overheating, if present, was too weak to be evaluated.

The temperature increase, ΔT, vs time, for each isothermal test, is reported in Figure 2. In this 3D plot the difference in the crystallization kinetic behavior at high and low temperatures is quite evident, and the height of the peaks is also reported as a gradient color in the blue base plane (logarithmic gradient: base = blue, maximum height = red). The complete set of isothermal tests is also reported in the Supporting Information.

According to Figure 2, the isothermal crystallization from the melt state exhibits a "double" kinetic behavior as recently observed:[24−26] interestingly, the data sets show a distinct turnabout at 45 °C. The mesophase crystallization occurs during sample cooling scans in the temperature range of 0−40 °C;[20] the observation of this behavior is definitely not an artifact.

Nevertheless, "crystallization times" have only an indirect relevance to practical heat-treatment processes because they are derived specifically for transformation under isothermal conditions. In practice, heat-treatment processes are usually concerned with transformations that occur during nonisothermal conditions, mostly continuous cooling. Indeed, the ability to predict the

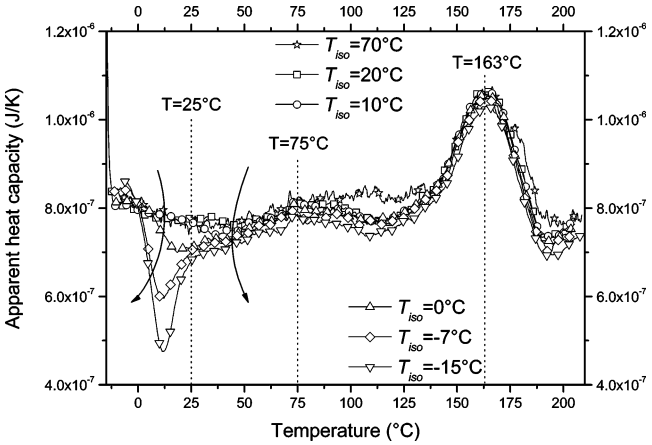

Figure 3. Selected thermograms of the i-PP sample (isothermally held at −15, −7, 0, 10, 20, and 70 °C for 1.5 s) at a heating rate of 50 K/s.

transformation kinetics under such conditions is of enormous practical significance.

A "double" behavior of the isothermal crystallization rates was also already observed for other semicrystalline polymers. Pyda et al.[27] observed in the detailed thermal analysis of poly(butylene terephthalate) (PBT), also based on superfast chip calorimetry, the bimodal shape of the isothermal crystallization rates. They suggested a mechanism change with the nature of the amorphous layer adjacent to the crystal, or naturally, a change in mechanisms due to a change in crystal structure or morphology.[27]

Supaphol and Spruiell[28] investigated the isothermal melt crystallization kinetics in syndiotactic polypropylene (s-PP) by the means of differential scanning calorimetry. In their work[28] the crystallization half times obtained by isothermal crystallization from the melt state exhibits a "double" bellshaped curve, as a function of temperature. They explained that, for the crystallization from the melt state of s-PP, the crystallization process is dominated by heterogeneous nucleation mechanisms until the crystallization temperature drops as low as 60 °C; at which point the contribution from the homogeneous nucleation mechanisms start taking effect and increasingly dominates with a further decrease in crystallization temperature (or further increase in the degree of undercooling).[28]

Subsequent Heating Behaviors. The i-PP morphologies, resulting from the solidification described in the previous section, namely, performed in a wide range of isothermal conditions, were investigated by subsequent heating. As schematized in Figure 1, after isothermal step of 1.5 s, the sample was cooled to −15 °C with the rate of 1000 K/s. The sample, after being held 0.1 s at −15 °C, was heated again in the nanocalorimeter at 50 K/s.

The thermograms of some of these selected scans performed at a heating rate of 50 K/s are shown in Figure 3. These thermograms, after solidification at an isothermal temperature from −15 to 20 °C, are consistent with the similar heating scans of samples solidified at a high cooling rate reported in ref 20. Indeed, only one well-defined endothermic peak at 163 °C is observed in the thermograms of the heating scans performed after solidification. This peak is obviously due to the melting of the α-monoclinic phase, also usually observed in the heating of samples crystallized in the α-monoclinic phase in standard calorimetry.

This process is preceded by a chain reorganization process (melting−recrystallization) from the mesomorphic phase to the α-monoclinic phase,[20] and it is not present in the sample crystallized at 70 °C during the isothermal step to the α-monoclinic phase. The net enthalpic effect accounts for the superposition of two large transitions, from 70 to 130 °C, with opposite signs occurring almost simultaneously, hiding each other's contributions (reorganization[16,18,27]), and appears small with respect to the area of the α melting peak. Recently, Cao and Sbarski tried to quantify the enthalpy of the solid-phase transition for i-PP fibers using a modified DSC technique.[29]

Reorganization and stability of the mesomorphic phase are also recently the subject of morphological studies of quenched samples.[30,31] The morphology of the mesomorphic i-PP in the nanoscopic scale is characterized by the so-called "nodule" of polygonal or spherical shape as was observed by transmission electron microscope (TEM).[32−34] The diameter of the nodule is approximately 10 nm at room temperature. The internodular distance confirmed by small-angle X-ray scattering (SAXS) measurement roughly corresponds to the diameter of the nodule observed by TEM.[32]

Zia et al.[31] suggest that the mesomorphic-to-monoclinic transition in nodular crystals at about 70 °C is not accompanied by complete melting of the domains and recrystallization, rather it seems to occur at the local scale within existing domains.

The thermograms of the heating scans, performed after isothermal crystallization at temperatures lower than 20 °C, show an exothermic event, between 0 and 30 °C (center position at 7 °C), and at higher temperature they join all other thermograms and closely follow the path of the isotherm at 20 °C, which had crystallized toward the mesomorphic phase. This exothermic event is related with a cold crystallization process to form the mesomorphic phase.[35,36,20]

The intensity (area) of the crystallization peak, between 0 and 30 °C, increases on decreasing the isothermal test temperature, applied during previous solidification, below 20 °C. This could be consistent with the observation that, during the corresponding isotherms, crystallization toward the mesomorphic phase was completed but the final degree of crystallinity is dependent on the time and the temperature at which crystallization is carried out.

The temperature range of the mesomorphic crystallization peak corresponds to the low-temperature peak of the mesomorphic crystallization processes shown in Figure 7 of ref 20, for cooling rates larger than 160 K/s. The peak width of about 20 K, between 0 and 30 °C, at the heating rate of 50 K/s implies that at those temperatures the kinetics are already fast enough to exhaust the crystallization process within a crystallization time of the order of a few tenths of a second.

The thermograms of some selected scans performed at a heating rate of 50 K/s, after solidification at an isothermal temperature 0 °C for different times and then cooled to −15 C at 1000 K/s, are shown in Figure 4.

Although no local overheating is apparently detected during the isothermal step at 0 °C, the effect of the increasing isothermal time is evident. If the isothermal step lasts 0.2 s, the thermogram shows an exothermic event, as in Figure 3, the cold crystallization process to form the mesomorphic phase between 0 and 30 °C (center position at 7 °C). On the increase of the isothermal step duration from 0.5 to 2.0 s, this exothermic event decreases until deviations are not evident in the thermograms corresponding to the isotherms lasting 2.0 and 4.0 s. This behavior suggests that isothermal crystallization at 0 °C, toward the mesophase, needs about 2 s.

Kinetic Analysis. The peak observed in temperature evolution during isothermal experiments is related to crystallization. The kinetics of first-order phase transitions driven by nucleation and growth kinetics are statistically described by the Kolmogorov−

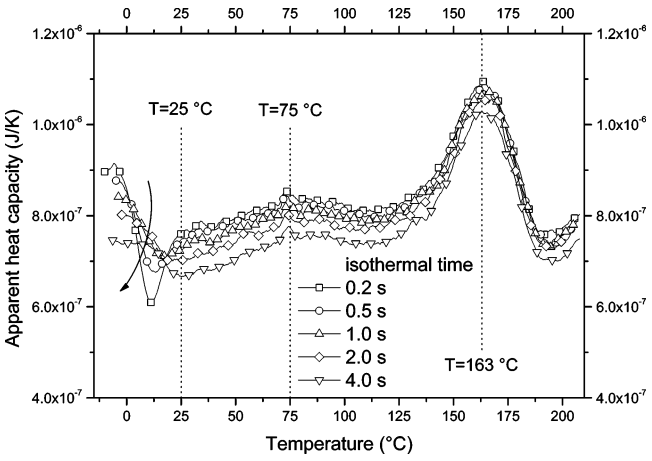

Figure 4. Selected thermograms of the i-PP sample (maintained at 0 °C for 0.2, 0.5, 1.0, 2.0, and 4.0 s) at a heating rate of 50 K/s.

Johnson−Mehl−Avrami theory.[37−42] Kolmogorov's probabilistic argument relates the crystallized fraction, ξ, to the extended crystallized fraction, φ_0, obtained by assuming that all growth centers continue unimpeded, by

$$\frac{d\xi}{(1-\xi)} = d\varphi_0 \tag{1}$$

in which the correcting factor $(1 - \xi)$, also known as the impingement factor, is nothing else but the volume fraction still available for crystallization. According to the classic form, the transformed volume fraction, ξ, as a function of time t can be evaluated according to the formula

$$\xi(t) = 1 - \exp[-\varphi_0(t)] \tag{2}$$

Obviously in the case of i-PP, both ξ and φ_0 have to be intended as total crystallized fractions, solidified to the α and the mesomorphic phase. Furthermore, the KJMA model can be expressed as the parallel of every single phase transformation,[43] relating each extended crystallized fraction to the proper nucleation and growth rate.

According to the Avrami form, the KJMA model can be also written as

$$\xi(t) = 1 - \exp[-k^n(t - t_0)^n] \tag{3}$$

or in the differential form

$$\xi_t(t) = \frac{d\xi}{dt} = nk^n(t - t_0)^{n-1} \exp[-k^n(t - t_0)^n] \tag{4}$$

$$\xi = 0 \quad \forall t \le t_0 \tag{5}$$

where k, n and t_0 are the crystallization rate constant, the Avrami index, and the initial time of the transformation, with the initial condition, eq 5.[44]

The time to transform half of the volume, $t_{1/2}$, is related to the rate constant, k, by

$$t_{1/2} = \frac{[\ln(2)]^{1/n}}{k} \tag{6}$$

The experimental temperature evolution can be linked to the crystallization process, assuming that it is the result of sharp exponential temperature decay due to the change from cooling to isothermal conditions[20] followed by an overheating due to crystallization:

$$T(t) - T_{iso} = \underbrace{(T_0 - T_{iso}) \times \exp\left(-\frac{t}{\tau}\right)}_{cooling} + \underbrace{A \times \xi_t(t)}_{crystallization} \tag{7}$$

where T_{iso} is the isothermal test temperature, T_0 is the sample temperature at the instant when the programmed temperature reaches T_{iso} (active cooling switches to ballistic cooling), and A is the peak area. The parameters τ, n, k, and A of the temperature evolution, eqs 6 and 7, were determined by nonlinear regression for each test temperature.[45]

The comparison between experimental temperature evolution and the fit according to eq 7 of the isotherms performed at the temperatures of 35 and 55 °C is shown in Figures 5 and 6. It is worth noticing that calculated temperatures fairly follow the experimental ones. In order to determine the quality of the fit, the residual plots are also shown in the insets of Figures 5 and 6. Residuals are the vertical difference between the actual data points and the fit curve. No large deviations from randomly scattered residuals around zero are observed, and the plots show no discernible pattern, i.e., eq 7 describes all parts of the experimental data similarly well (the complete series of calculated temperatures evolutions are reported in ref 45, with tabled fitting parameters and results[45]).

The Avrami exponent value depends on the dimensionality of the growth process and on the kind of nucleation. Furthermore, although the fit is not very sensitive to the Avrami index, the best fitting (minimizing residual sum of squares, RSS) is obtained with $n = 4$ for the isothermal tests for temperature lower than 45 °C, as shown in Figure 5 for the isothermal test at 35 °C. The crystallization kinetics of the mesophase at a temperature of 35 °C, interpreted through the Kolmogorov model with an Avrami exponent $n = 4$, suggests to be the result of a three-dimensional growth combined with homogeneous nucleation.

On the other hand, for isothermal tests for temperatures higher than 45 °C, as shown in Figure 6 for the isothermal test at 55 °C, the quality of the fit for $n = 3$ is comparable to that obtained for $n = 4$. In most common cases observed for the α phase crystallization, where three-dimensional growth is combined with heterogeneous nucleation, the Avrami exponent, n, assumes the value of 3.

The result of the kinetic analysis, i.e., the reciprocal crystallization rate constant k, is reported in Figure 7. The same plot also shows a large number of kinetic data available in the literature concerning the isothermal crystallization of i-PP,[46−66] obtained from experiments collected with various methods. Despite the scatter, the results, plotted in Figure 7, clearly indicate a concentrated band from 110 to 160 °C, partially covered also by standard isothermal calorimetry on the same resin.

The kinetic data, obtained by interpreting nanocalorimetry isothermal results obtained in this work, cover a range of temperatures from 5 to 85 °C, mostly of that unexplored previously. On the other hand, they also match well with some polarized light microscopy data by Magill,[49] as well as with the general trend of isothermal literature data.[46−66] In Figure 7, it is evident that at temperatures lower than 45 °C, there is a variation in the kinetic behavior: we think that below 45 °C, the mesophase is formed by homogeneous nucleation (Avrami index $n = 4$) and above 45 °C, the α phase prevails due to heterogeneous nucleation (Avrami index $n = 3$). In both cases, three-dimensional crystal growth is assumed.

Conclusions

In this paper the isothermal crystallization of an i-PP, with subsequent heating, was obtained by a novel nanocalorimeter,

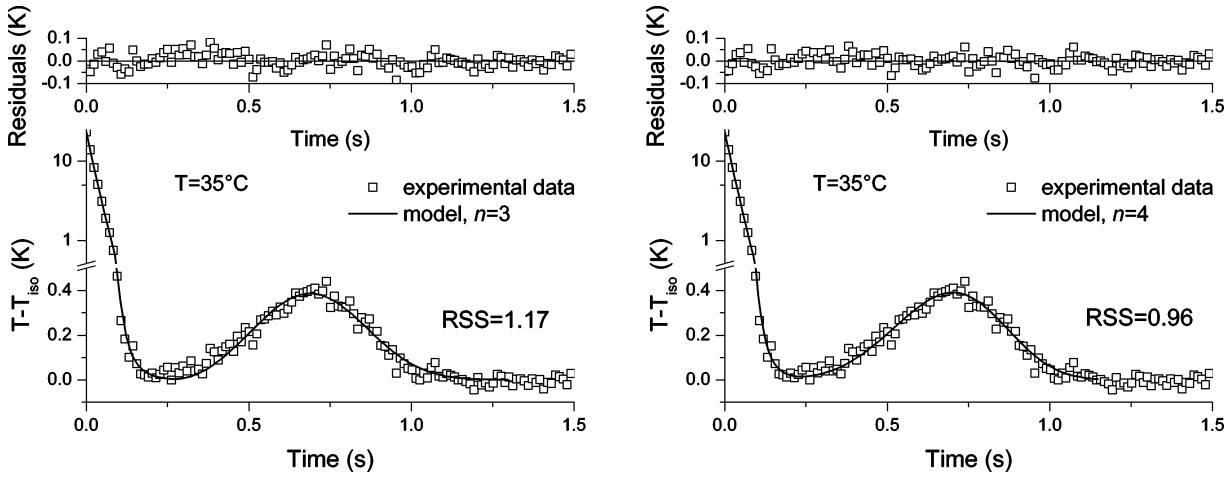

Figure 5. Experimental temperature evolution and fit (left plot with $n = 3$, right plot with $n = 4$), according to eq 7, of the isotherm performed at the temperature of 35 °C. The inset shows the difference between experimental and fit curves (residuals).

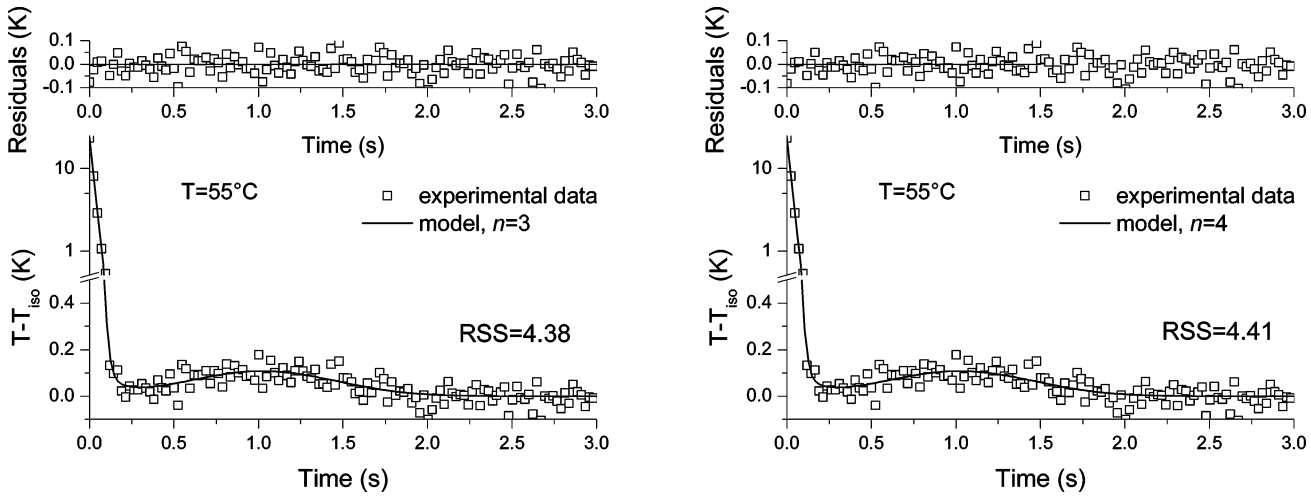

Figure 6. Experimental temperature evolution and fit (left plot with $n = 3$, right plot with $n = 4$), according to eq 7, of the isotherm performed at the temperature of 55 °C. The inset shows the difference between experimental and fit curves (residuals).

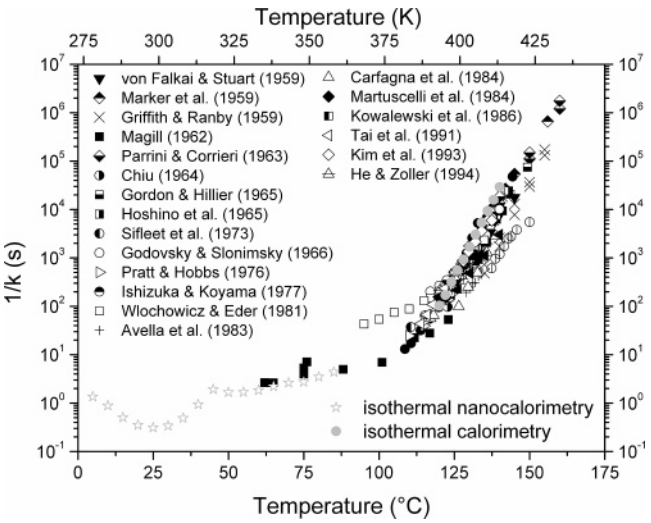

Figure 7. Cumulative data of the isothermal crystallization of i-PP: variation of the reciprocal crystallization rate constant k as a function of crystallization temperature. Black symbols: literature data. Isothermal nanocalorimetry and isothermal calorimetry as gray stars and circles, respectively.

which can adopt samples having mass of the order of 100 ng and of about 10 μm thickness.

Many isothermal crystallization experiments were carried out from 90 to −15 °C after cooling from the melt performed at a high cooling rate (1000 K/s); after each isothermal step the polymer was heated with a heating rate of 50 K/s.

The temperature evolutions of the isothermal steps confirm that crystallization kinetics exhibit a "double" kinetic behavior; recently observed on i-PP.[24−26]

The data sets show a distinct trend change at 45 °C, suggesting that the well-known α-monoclinic crystalline phase forms when the i-PP is solidified at temperatures higher than 45 °C, and mesophase crystallization kinetics prevails at temperatures lower than 45 °C.

The "double" kinetic behavior, shown by the isothermal tests, is confirmed by the behavior during subsequent heating runs, after isothermal solidification, which in addition show that (i) on heating at a rate of 50 K/s, the mesomorphic phase transforms into the α-monoclinic phase in the interval 70−130 °C; (ii) the thermograms of the heating scans, performed after isothermal crystallization at temperature lower than 20 °C, show an exothermic event, in the temperature interval 0−30 °C consistent with a cold crystallization process to form the mesomorphic phase.

The peaks observed in temperature evolution during isothermal experiments can be fitted using the Kolmogorov−Johnson−Mehl−Avrami model, and the Avrami index suggests that the crystallization kinetics of the mesophase, at a temperature of 35 °C, is attained with homogeneous nucleation.

Finally, the crystallization kinetics constant, obtained in the range 5−85 °C through the KJMA model, is compared with literature results. The crystallization of i-PP, at temperatures lower than 45 °C, reveals a different kinetic behavior related to the mesophase development.

Acknowledgment. One of the authors (F.D.S.) is grateful for a COST grant (Grant COST-STSM-P12-00437). The main experimental part of this work was carried out during a short-term scientific mission (STSM) at Rostock University within the COST action P12 "Structuring of Polymers". This work was supported also by the Ministero dell'Istruzione, dell'Università e della Ricerca (Grant Prin 2004 titled "Control and Modeling of Morphology of Semicrystalline Polymers under Realistic Processing Conditions").

Supporting Information Available: Figures of all the experiments showing the results of isothermal tests. This material is available free of charge via the Internet at http://pubs.acs.org.

References and Notes

(1) Gatos, K. G.; Minogianni, C.; Galiotis, C. *Macromolecules* **2007**, *40*, 786−789.
(2) Addink, E. J.; Beintema, J. *Polymer* **1961**, *2*, 185−193.
(3) Vittoria, V. In *Handbook of Polymer Science and Technology*; Cheremisinoff, N. P., Ed.; Marcel Dekker: New York, 1989; Vol. 2, p 507.
(4) Brückner, S.; Meille, S. V.; Petraccone, V.; Pirozzi, B. *Prog. Polym. Sci.* **1991**, *16*, 361−404.
(5) Alberola, N.; Fugier, M.; Petit, D.; Fillon, B. *J. Mater. Sci.* **1995**, *30*, 860−868.
(6) Corradini, P.; Petraccone, V.; De Rosa, C.; Guerra, G. *Macromolecules* **1986**, *19*, 2699−2703.
(7) Natta, G.; Peraldo, M.; Corradini, P. *Atti. Accad. Naz. Lincei, Cl. Sci. Fis., Mat. Nat., Rend.* **1959**, *26*, 14−17.
(8) Miller, R. L. *Polymer* **1960**, *1*, 135−143.
(9) Glotin, M.; Rahalkar, R. R.; Hendra, P. J.; Cudby, M. E. A.; Willis, H. A. *Polymer* **1981**, *22*, 731−735.
(10) Coccorullo, I.; Pantani, R.; Titomanlio, G. *Polymer* **2002**, *44*, 307−318.
(11) Sorrentino, A.; De Santis, F.; Titomanlio, G. *In Progress in Understanding of Polymer Crystallization*; Reiter, G., Strobl, G., Eds; Springer: Berlin, Heidelberg, Germany, 2007; p 343.
(12) Pijpers, T. F. J.; Mathot, V. B. F.; Goderis, B.; Scherrenberg, R. L.; van der Vegte, E. W. *Macromolecules* **2002**, *35*, 3601−3613.
(13) Saunders, M.; Podluii, K.; Shergill, S.; Buckton, G.; Royall, P. *Int. J. Pharm.* **2004**, *274*, 35−40.
(14) Wilthan, B.; Cagran, C.; Pottlacher, G. *Int. J. Thermophys.* **2005**, *26*, 1017−1029.
(15) Adamovsky, S. A.; Minakov, A. A.; Schick, C. *Thermochim. Acta* **2003**, *403*, 55−63.
(16) Minakov, A. A.; Mordvintsev, D. A.; Schick, C. *Polymer* **2004**, *45*, 3755−3763.
(17) Adamovsky, S.; Schick, C. *Thermochim. Acta* **2004**, *415*, 1−7.
(18) Minakov, A. A.; Mordvintsev, D. A.; Schick, C. *Faraday Discuss.* **2005**, *128*, 261−270.
(19) Minakov, A. A.; Morikawa, J.; Hashimoto, T.; Huth, H.; Schick, C. *Meas. Sci. Technol.* **2006**, *17*, 199−207.
(20) De Santis, F.; Adamovsky, S.; Titomanlio, G.; Schick, C. *Macromolecules* **2006**, *39*, 2562−2567.
(21) Lamberti, G.; De Santis, F.; Brucato, V.; Titomanlio, G. *Appl. Phys. A: Mater. Sci. Process.* **2004**, *78*, 895−901.
(22) Pantani, R.; Speranza, V.; Coccorullo, I.; Titomanlio, G. *Macromol. Symp.* **2002**, *185*, 309−326.
(23) De Santis, F.; Ferrara, M.; Neitzert, H. C. *IEEE Trans. Instrum. Meas.* **2006**, *55*, 123−127.
(24) General Discussion. *Faraday Discuss.* **2005**, *128*, 321−339.
(25) Silvestre, C.; Cimmino, S.; Duraccio D.; Schick C. *Macromol. Rapid Commun.* **2007**, *28*, 875−881.
(26) Ray, V. V.; Banthia, A. K.; Schick C. *Polymer* **2007**, *48*, 2404−2414.
(27) Pyda, M.; Nowak-Pyda, E.; Heeg, J.; Huth, H.; Minakov, A. A.; Di Lorenzo, M. L.; Schick, C.; Wunderlich, B. *J. Polym. Sci., Part B: Polym. Phys.* **2006**, *44*, 1364−1377.
(28) Supaphol, P.; Spruiell, J. E. *Polymer* **2001**, *42*, 699−712.
(29) Cao, J.; Sbarski, I. *Polymer* **2006**, *47*, 27−31.
(30) Konishi, T.; Nishida, K.; Kanaya, T. *Macromolecules* **2006**, *39*, 8035−8040.
(31) Zia, Q.; Androsch, R.; Radusch, H. J.; Piccarolo, S. *Polymer* **2006**, *47*, 8163−8172.
(32) Hsu, C. C.; Geil, P. H.; Miyaji, H.; Asai, K. *J. Polym. Sci., Part B: Polym. Phys.* **1986**, *24*, 2379−2401.
(33) Ogawa, T.; Miyaji, H.; Asai, K. *J. Phys. Soc. Jpn.* **1985**, *54*, 3668−3670.
(34) Grubb, D. T.; Yoon, D. Y. *Polym. Commun.* **1986**, *27*, 84−88.
(35) Caldas, V.; Brown, G. R.; Nohr, R. S.; MacDonald, J. G.; Raboin, L. E. *Polymer* **1994**, *35*, 899−907.
(36) Miyamoto, Y.; Fukao, K.; Yoshida, T.; Tsurutani, N.; Miyaji, H. *J. Phys. Soc. Jpn.* **2000**, *69*, 1735−1740.
(37) Kolmogorov, A. N. *Bull. Acad. Sci. USSR, Mater. Ser.* **1937**, *1*, 355−359.
(38) Johnson, W. A.; Mehl, R. F. *Trans. Am. Inst. Min., Metall. Pet. Eng.* **1939**, *135*, 416−458.
(39) Avrami, M. *J. Chem. Phys.* **1939**, *7*, 1103−1112.
(40) Avrami, M. *J. Chem. Phys.* **1940**, *8*, 212−224.
(41) Avrami, M. *J. Chem. Phys.* **1941**, *9*, 177−184.
(42) Avrami was a European chemist, Johnson and Mehl, US metallurgists, and Kolmogorov, a Russian mathematician. So Europeans, polymer scientists, and chemical engineers tended to call these equations "Avrami". Metallurgists and Americans: Johnson−Mehl−Avrami or JMA. After the Cold War, Kolmogorov's paternity is fully recognized, and KJMA or JMAK are now both used.
(43) Matsuda, H.; Bhadeshia, H. K. D. H. *Mater. Sci. Technol.* **2003**, *19*, 1330−1334.
(44) Lorenzo, A. T.; Arnal, M. L.; Albuerne, J.; Müller, A. J. *Polym. Test.* **2007**, *26*, 222−231.
(45) De Santis, F.; Adamovsky, S.; Titomanlio, G.; Schick, C. In preparation.
(46) von Falkai, B.; Stuart, H. A. *Kolloid−Z.* **1959**, *162*, 138−140.
(47) Griffith, J. H.; Ranby, B. G. *J. Polym. Sci.* **1959**, *38*, 107−116.
(48) Marker, L.; Hay, P. M.; Tilley, G. P.; Early, R. M.; Sweeting, O. J. *J. Polym. Sci.* **1959**, *38*, 33−43.
(49) Magill, J. H. *Polymer* **1962**, *3*, 35−42.
(50) Parrini, P.; Corrieri, G. *Makromol. Chem.* **1963**, *62*, 83−96.
(51) Chiu, J. *Anal. Chem.* **1964**, *36*, 2058−2061.
(52) Gordon, M.; Hillier, I. H. *Polymer* **1965**, *6*, 213−219.
(53) Hoshino, S.; Meinecke, E.; Powers, J.; Stein, R. S. *J. Polym Sci, Part A* **1965**, *3*, 3041−3065.
(54) Sifleet, W. L.; Dims, N.; Collier, J. R. *Polym. Eng. Sci.* **1973**, *13*, 10−16.
(55) Godovsky, Y. K.; Slonimsky, G. L. *J. Polym Sci.* **1974**, *12*, 1053−1080.
(56) Pratt, C. F.; Hobbs, S. Y. *Polymer* **1976**, *17*, 12−16.
(57) Ishizuka, O.; Koyama, K. *Polymer* **1977**, *18*, 913−918.
(58) Wlochowicz, A.; Eder, M. *Polymer* **1981**, *22*, 1285−1287.
(59) Rybnikar, F. *J. Appl. Polym. Sci.* **1982**, *27*, 1479−1486.
(60) Avella, M.; Martuscelli, E.; Pracella, M. *J. Therm. Anal.* **1983**, *28*, 237−248.
(61) Carfagna, C.; De Rosa, C.; Guerra, G.; Petraccone, V. *Polymer* **1984**, *25*, 1462−1464.
(62) Martuscelli, E.; Pracella, M.; Volpe, G. D.; Greco, P. *Makromol. Chem.* **1984**, *185*, 1041−1061.
(63) Kowalewski, T.; Galeski, A. *J. Appl. Polym. Sci.* **1986**, *32*, 2919−2934.
(64) Tai, H.-J.; Chiu, W.-Y.; Chen, L.-W.; Chu, L.-H. *J. Appl. Polym. Sci.* **1991**, *42*, 3111−3122.
(65) Kim, C. Y.; Kim, Y. C.; Kim, S. C. *Polym. Eng. Sci.* **1993**, *33*, 1445−1451.
(66) He, J.; Zoller, P. *J. Polym. Sci., Part B: Polym. Phys.* **1994**, *32*, 1049−1067.

MA071491B